

## Finite Element Analysis of Tin-Bismuth Electromigration of Solder Joints

Mehdi Hamid, Prabjit Singh, Tom Wassick  
IBM Corporation  
MN, USA

Haley Fu  
iNEMI  
Shanghai, China

Raiyo Aspandiar  
Intel Corporation  
OR, USA  
Mehdi.Hamid@ibm.com

### ABSTRACT

Electromigration is a mass transport phenomenon involving diffusion, electric current, mechanical stress and temperature gradients. Atomic movement from cathode to anode in metal lines subjected to high current density causes voiding on the cathode side and hillocks on the anode side of solder joints. The movement of atoms towards the anode causes back stress that counters electromigration to the extent that it may stop electromigration in very short solder joints. The need for a low melting point solder, lower printed circuit board and component warpage, eco benefits (green technology) and lowering reflow temperature to accommodate components which can't withstand tin, silver and copper alloy solders reflow temperatures have been leading the microelectronic industry towards Sn-Bi alloys. In this work a finite element model was developed to predict the resistance of a Sn-Bi solder joint to electromigration and to determine the temperature, current density, and mechanical stress distribution in a solder joint. A novel empirical electromigration test method is introduced that can estimate the temperature of the solder joint before and after the electromigration test. The modeling and test results are compared and discussed.

Key words: Solder Joint, Electromigration, Finite Element Analysis, Tin Bismuth alloys, Coupled Physics

### INTRODUCTION

The use of lead in solders in electrical and electronic equipment was severely restricted by the Restriction of Hazardous Substances Directive 2002/95/EC (RoHS) adopted by the European Union in February 2003. As a result, industry had to select a lead-free solder. Early in the selection process, tin-bismuth eutectic alloy was a leading candidate, but the heavy loading of components with lead-

containing component terminations excluded tin-bismuth from the list of desirable solders, because of its reaction with lead-containing solders forming a low melting ternary eutectic. The industry moved to SAC (Sn, Ag and Cu containing alloy) solder, instead. Now that components with lead-containing termination metallurgies have been flushed out of the supply chain, Sn-Bi eutectic solder is gaining market share in electronic assemblies. The main advantage of Sn-Bi is its lower melting point that results in less warpage of the soldered assemblies. Other advantages that the reduced energy consumption during soldering and the lower cost of substrates and component packaging that do not need to survive higher processing temperatures.

Given the very high homologous temperature of Sn-Bi eutectic at ambient temperatures, its metallurgy is constantly changing at noticeable rates, even at room temperature. In addition, the Bi atoms with their very high effective valence being much higher than the Sn atoms, migrate and segregate at the anode side of the solder joint. A layer of almost pure Bi forms at the anode raising the electrical resistance of the joint. The brittle nature of bismuth may also make the solder joints with segregated Bi more prone to fracture from shock and vibration.

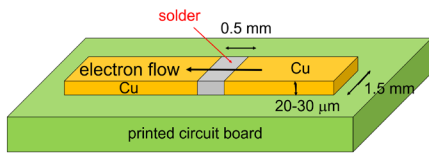
Electromigration remains a major reliability issue at all levels of electronic packaging technology mainly because of the ever-reducing device and package sizes and increasing current densities. Hillocks and voids that form on and in solder joints at high current densities can lead to short and open circuits. It is well known that electromigration is caused by electron wind force. However, there are other driving forces at work during electromigration. One such force is the back stress, discovered by Blech who showed that stress builds up in metal films subjected to electromigration that

opposes further electromigration [1-3]. Kirchheim et al [4-5] and Korhonen were able to further derive equations for vacancy transport and stress propagation based on vacancy generation and annihilation.

Much research has been published on electromigration testing and on numerical analysis explaining the experimental results. [6-8]. In this work a 3D finite element analysis of electromigration in Sn-Bi solder is presented and the modeling results are compared and verified with testing.

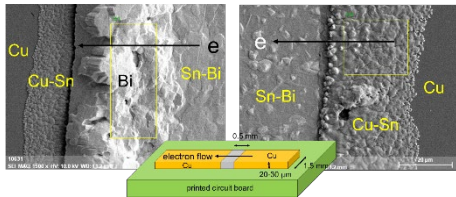
### TESTING

Electromigration in ball-grid-array (BGA) and controlled collapse chip connection (C4) solder joints have been studied by monitoring the electrical resistance of the joints followed by post-test cross sectioning of the joints, a destructive technique. This paper is based on a novel approach we term the planar solder joint approach which affords non-destructive real-time monitoring of the solder joint microstructure in a scanning electron microscope. The planar solder joints are typically 0.15 to 0.5 mm long, 1 to 1.5 mm wide and 30 mm thick. They are fabricated by laying a solder coated strip of copper, about 0.1 mm thick over the copper lines to be joined by the solder. The solder under the copper strip is reflowed while the strip is pressed against the circuit board and kept pressed while the solder solidifies. The copper strip is then ground off using 600-grit paper, followed by the polishing of the solder bridge that is now the solder planar joint bridging the gap in the copper lines. Figure 1 is a schematic of the fabricated planar solder joint test specimen.



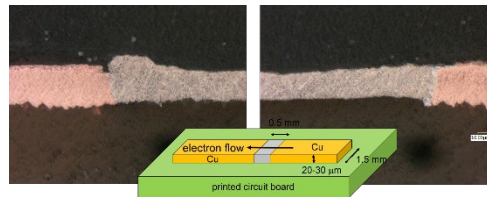
**Figure 1.** Illustration of the planar solder joint between copper lines

Figure 2, SEM micrograph looking down on the joint showing hillock formation of Bi-rich phase at the anode and loss of Bi at the cathode.



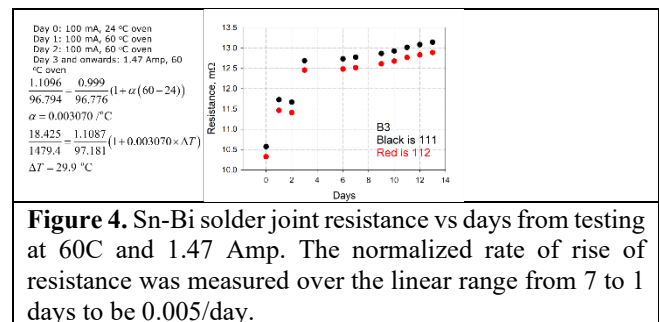
**Figure 2.** SEM micrograph of a Planar Sn-Bi solder joint after 1 Amp has been flowing through for 8 days at 100 °C at a current density of 3.4 kA/cm<sup>2</sup>. The left micrograph shows the anode end of the joint and the right micrograph shows the cathode end

Figure 3 shows cross sectional view of a planar solder joint between two copper lines.



**Figure 3.** Planar solder joint in cross section after substantial electromigration. Notice the hillock formation at the anode end to the left which has result to solder buildup

Electromigration tests were run in 60 and 80 °C ambient. The first step in the electromigration test runs was to obtain data that would be used to predict the temperature of the solder joint during the electromigration run. Let us use the 60 °C run as an example to explain the estimation of the solder joint temperature during the electromigration run at 1.47 Amp , 2.9 kA/cm<sup>2</sup> current density. Figure 4 shows that the test run has four periods: (1) Day 0 at 100 mA current at room temperature of 24 °C; (2) Day 1 and 2 at 100 mA current at 60 °C ambient; (3) Day 3 and beyond at 1.47 Amp current at 60 °C ambient. The joule heating at 100 mA current is negligible and therefore can be used to determine the temperature coefficient of resistivity of the solder. We obtained the temperature coefficient (a) of resistivity to be 0.0031 /°C and using this a we obtained the solder joint temperature during the electromigration run to be 90 °C. From the slope of the resistance vs days curve of Figure 4, we obtained the rate at which electromigration progressed which we express in terms of normalized rate of rise of resistance of 0.005/day. The normalized rate of rise of resistance is the rate of resistance divided by the initial resistance.



**Figure 4.** Sn-Bi solder joint resistance vs days from testing at 60C and 1.47 Amp. The normalized rate of rise of resistance was measured over the linear range from 7 to 14 days to be 0.005/day.

### Modeling

A half symmetry Sn-Bi solder was designed using Ansys SpaceClaim CAD tool [9] with 0.5 mm long, 1 mm width and 15 μm thickness geometry shown in Figure 5. Two copper conductors were designed on top, and bottom of the solder joint. The copper conductors width, height and length dimensions were designed as 35 μm x 50 μm x 1.25 mm respectively.

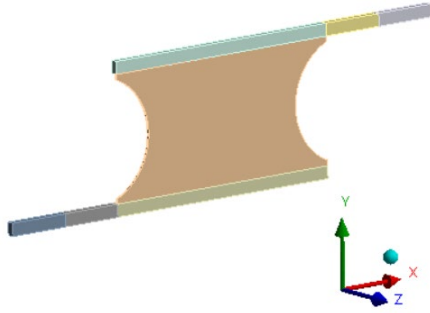


**Figure 5.** Half symmetry (in Z direction) solder joint with Cu conductors on top and bottom

A coupled physics based finite element model for solder joint with copper conductors were defined using diffusion, electric current, stress gradient and temperature gradient formulations.

### Governing equations

Atomic migration in metallic interconnects is driven by several forces like electrostatic force, electron wind through electric current and by gradients of atomic concentration (diffusion), hydrostatic stress (stress migration) and temperature (thermos-migration). Fick's first law of diffusion was implemented (Eq. 1) to include all these driving forces in the current electromigration model.

$$J_a = \frac{[D]}{K T} C \nabla \mu \quad \text{Eq.1}$$

Where [D] is atomic diffusivity matrix, K is Boltzmann's constant, T is the absolute temperature, and  $\mu$  is the generalized chemical potential derived from atomic concentration C, electric potential  $\rho$ , hydrostatic stress ( $\sigma_H$ ) and temperature.

**Table 1.** Driving forces of electromigration

Process	Chemical potential $\mu$	Force $F = -\nabla \mu$	Flux $J = \left(\frac{D}{KT}\right) c F$
<b>Diffusion</b>	$kT \ln C$	$-kT \frac{\nabla C}{C}$	$-D \nabla C$
<b>Electromigration</b>	$Z^* e \phi$	$-Z^* e \nabla \phi$	$-\left(\frac{D}{KT}\right) C Z^* e \nabla \phi$
<b>Stress migration</b>	$-\Omega \sigma_H$	$\Omega \nabla \sigma_H$	$\left(\frac{D}{KT}\right) C \Omega \nabla \sigma_H$
<b>Thermomigration</b>	$\left(\frac{Q}{T}\right) T$	$-\left(\frac{Q}{T}\right) \nabla T$	$\left(\frac{D}{KT^2}\right) C Q \nabla T$

Including all the driving forces into Eq.1 from Table 1 we obtained the following equation.

$$J_a = -[D] \nabla C - \left(\frac{[D]}{KT}\right) C Z^* e \nabla \phi + \left(\frac{[D]}{KT}\right) C \Omega \nabla \sigma_H + \left(\frac{[D]}{KT^2}\right) C Q \nabla T \quad \text{Eq.2}$$

Where  $Z^*$  is effective charge number of the atom that combines the effect of electrostatic and the electron wind forces, e is electron charge,  $\Omega$  is the atomic volume, and Q is the heat of atomic transport. Also, hydrostatic stress ( $\sigma_H$ ) by definition is defined as the average of principal stresses.

By applying second Fick's law for mass balance and Newton's second law as well as thermal flux and electric current density to Eq.2 we obtained Eq.3.

$$J_a = -\left([D] + \frac{[D] C \Omega}{3KT} \text{tr}([c]\{\beta\})\right) \nabla C - \left(\frac{[D]}{KT}\right) C Z^* e \nabla \phi + \frac{[D] C \Omega}{3KT} \text{tr}([c](\nabla u)) - \left(\frac{[D]}{KT^2}\right) C Q + \frac{[D] C \Omega}{3KT} \text{tr}([c]\{\alpha\}) \nabla T \quad \text{Eq.3}$$

Where [c] is elasticity matrix,  $\{\alpha\}$  is vector of coefficient of thermal expansion,  $\{\beta\}$  is coefficient of diffusion expansion and u is a displacement vector.

A transient electromigration finite element analysis of a Sn-Bi solder joint under high electric current load is completed to show the combined coupled physics effect of diffusion, electromigration, stress migration, and thermomigration on the atomic concentration in solder joint.

The model was meshed using SOLID226 coupled filed elements. CONTA174 contact elements were defined between solder joint and copper conductors. Both elements have the following DOFs active: concentration (C), electric potential ( $\phi$ ), displacements ( $u_x, u_y, u_z$ ) and temperature (T). Also, an INFIN111 element was assigned to far end of each copper conductors to consider thermal conduction effect of wires connected to copper conductors during testing. INFIN111 element models an open boundary of a 3D unbounded field problem. A single layer of element is used to represent an exterior sub domain of semi-infinite extent [15]. Applied material properties of copper and Sn-Bi solder are shown in Table 2.

**Table 2.** Materials properties [10-14]

Material properties	Cu plates	Sn-Bi solder
Diffusion		
Diffusivity (pre-exponent) $D_0$ , $m^2/s$	$7.85 \times 10^{-5}$	$3.0 \times 10^{-9}$
Activation energy $E_a$ , J/mol	210	-
Activation energy $E_a$ , eV	-	0.58
Electric		
Electrical resistivity, Ohm.m	$2.33 \times 10^{-8}$	$35.1 \times 10^{-8}$
Effective charge number $Z^*$	-4	-17
Structural		
Young's modulus $E$ , Pa	$127 \times 10^9$	$38.4 \times 10^9$
Poisson's ratio	0.31	0.35
Thermal expansion $\alpha$ , 1/C	$17.1 \times 10^{-6}$	$1.5 \times 10^{-5}$
Diffusion expansion $\beta$	$1 \times 10^{-2}$	$2 \times 10^{-3}$
Atomic volume $\Omega$ , $m^3$	$1.182 \times 10^{-29}$	$2.71 \times 10^{-29}$
Thermal		
Thermal conductivity $k$ , W/(m.K)	393	57
Specific heat, J/(kg.K)	385.2	219
Density, kg/m <sup>3</sup>	8900	7390
Heat of transport $Q$ , eV	-	0.0094

An electric current of 1 A (0.5 A for half symmetry) was applied to one copper lead while the other lead is grounded (Figure 6a). The structural displacement  $u_z$  were constrained on the symmetry surface while  $u_y$  displacements were constrained at the top and bottom surfaces of the model to prevent the structure expansion in the vertical direction (Figure 5). A convection boundary condition with a film coefficient of  $62 \text{ W/m}^2\cdot\text{C}$  to an ambient temperature of  $83^\circ\text{C}$  was specified for all surfaces except the symmetry plane. A transient analysis was completed for Sn-Bi solder with  $83^\circ\text{C}$  ambient temperature. For applied electric current density of  $6.67 \text{ kA/cm}^2$  and ambient temperature of  $83^\circ\text{C}$  the transient analysis was completed for  $4.3 \times 10^4 \text{ s}$  (~ 12 h) to compare the result with experimental testing. Average current density distribution through the copper conductors and solder joint is shown in Figure 6b.

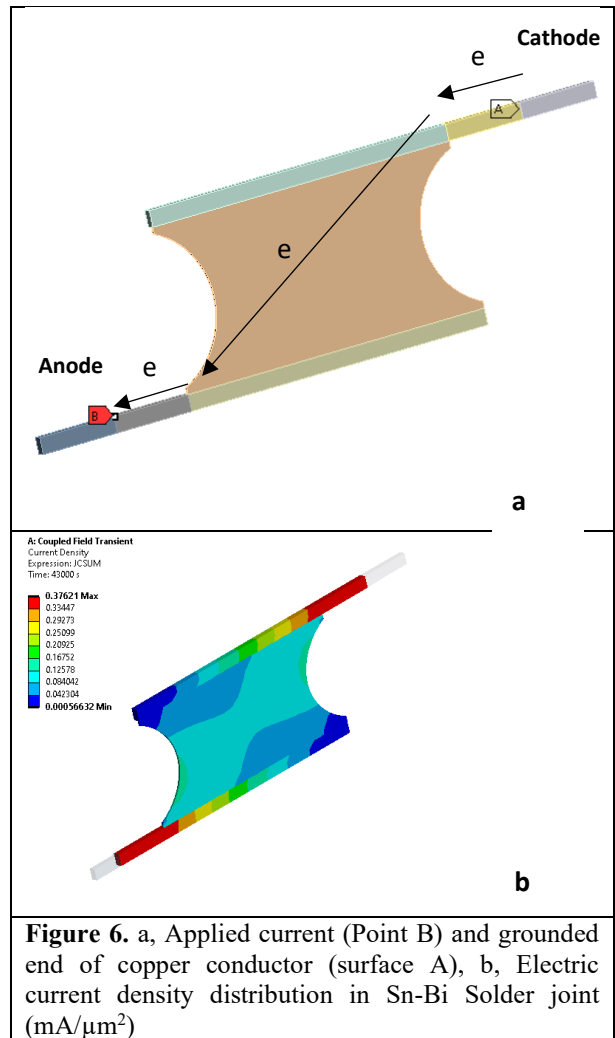


**Figure 6.** a, Applied current (Point B) and grounded end of copper conductor (surface A), b, Electric current density distribution in Sn-Bi Solder joint ( $\text{mA}/\mu\text{m}^2$ )

Normalized atomic concentration in solder joint is shown in Figure 7. Since the diffusion through the copper is very low the electromigration occurs at the interface between the solder and the copper plates.

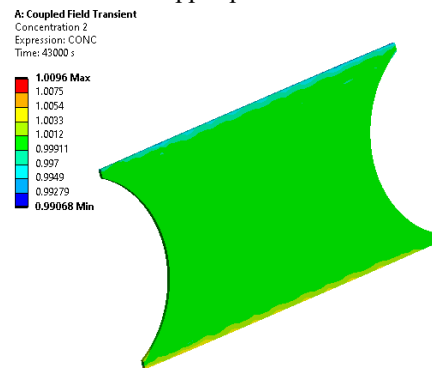


**Figure 7.** Normalized atomic concentration in solder joint

The distribution of normalized concentration (Figure 7) shows the atomic depletion regions are located at the material interfaces as well as in the solder joint. On the cathode side where the concentration is below 1 an atomic depletion is detected whereas on the anode side increase of atomic

concentration is detected which can be representation of early hillocks initiation. The non-uniform distribution of current density shown in Figure 6b led to non-uniform atomic concentration distribution, current crowding and Joule heating. Current crowding and Joule heating play crucial role in electromigration failure by increasing electromigration rate. Also, rapid migration of Cu atoms from cathode to anode creates several reliability issues involve the formation of voids, cracks, and damage at the cathode side, reduction in thickness of interfacial intermetallic compound (IMC) layer and rapid growth of interfacial IMC layer at the anode side. Additional downfall of these voids and cracks on the cathode side is decrease of cross section area of the solder contact which leads to increase of local current density and local electrical resistance [16].

The temperature distribution in Sn-Bi solder is shown in Figure 8 for about  $4.3 \times 10^4$  s simulation duration. A maximum temperature of  $97.6^\circ\text{C}$  was predicted by the model due to resistance increase and Joule heating effect. The applied electric current was 1 Amp and for the ambient temperature of  $83^\circ\text{C}$ .

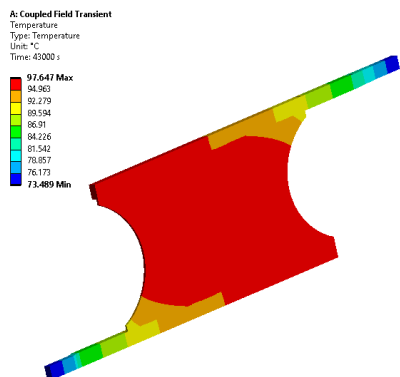


**Figure 8.** Temperature distribution on the solder joint after 12 hours

The increased temperature and temperature gradient on the solder joint contribute to atomic migration which led to stress gradients due to displacement constraints on the top and bottom surfaces of the model and thermal strain incompatibility between the solder and copper plates. The stress distribution in solder joint, Figure 9, shows a distribution of compressive stress in the majority of the solder joint other than sharp corners of the solder where there is higher rate of cooling.

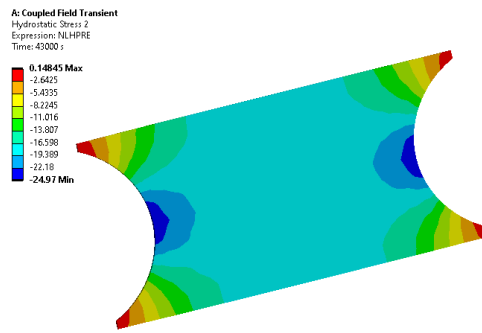


**Figure 9.** Hydrostatic stress (MPa) distribution in solder joint

The increase in total electrical resistance over time is shown in Figure 10. This increase is due to the dependency of local resistivity to concentration. The resistivity increase with concentration also affects the atomic transport. For a given current density,  $J$ , higher resistivity result in higher electric field density  $E = \rho J$  thus reinforcing the process of electromigration. A resistance of  $13.49 \text{ m}\Omega$  was predicted by the model which is in close agreement with measured resistance from testing of  $14.88 \text{ m}\Omega$ . It should be noted that the observed 10 % difference in solder joint predicted resistance can be related to solder joint geometry, some to Sn-Bi solder material properties as well as current density difference due to cross section mismatches between the model and actual solder joint-conductor cross section from testing. The testing part was completed in 5 consecutive stages. In stage one, which was about 2.5 h the electric current was set at 100 mA and oven temperature of  $24^\circ\text{C}$  where the initial resistance of  $11.2 \text{ m}\Omega$  was recorded. In second, third and fourth steps where each took about 2.5 h the electric current was kept constant at 100 mA however the oven temperature was raised gradually from  $24^\circ\text{C}$  at step one to  $41^\circ\text{C}$ ,  $61^\circ\text{C}$ , and  $83^\circ\text{C}$  in steps 2, 3 and 4 respectively. At the last step an electric current of 1 Amp was applied while the temperature was kept constant at  $83^\circ\text{C}$  for about 12 h. In Figure 10b, it is shown the resistance increase due to increase of temperature in steps 1 to 4 while the increase of resistance in last step is due to increase of electric current and Joule heating since the oven temperature was kept constant for the period of last step of testing. To calculate the temperature of solder joint in the last step with electric current of 1 Amp and oven temperature of  $83^\circ\text{C}$ , the temperature coefficient ( $\alpha$ ) of resistivity was calculated, as is explained in the testing section of this work, and shown in Figure 10c. The calculated temperature is about  $94^\circ\text{C}$  shown with the red data point in figure 10 c, which is in a close agreement with predicted max solder joint temperature from modeling of  $97.6^\circ\text{C}$ .

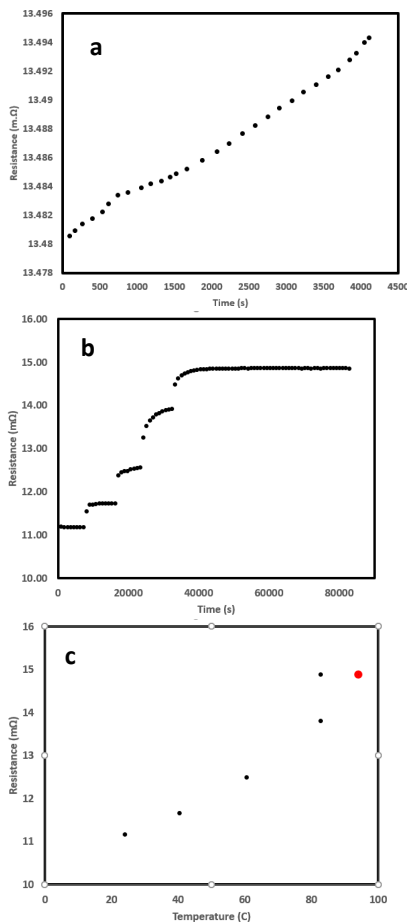


**Figure 10.** Electrical resistance vs time a, Modeling result b, Testing result c, Resistance vs temperature change over 5 steps of testing

## CONCLUSION

It is known that three factors that play major role in electromigration in Sn-Bi solder joints are current crowding, Joule heating and crystallographic orientation of the grains. In this study the effect of all three were analyzed. The effect of crystallographic orientation of Bi grains were implemented by calculating the activation energy of Bi grains in Sn-Bi alloy through experimental testing. Current crowding and Joule heating effects were implemented by employing governing equations for these physical phenomena. The predicted solder temperature due to electromigration and Joule heating was in a close agreement with measured solder joint temperature. Additionally, the solder resistance for the given ambient temperature and applied current was predicted to with 10 % margin of the measured resistance value. The reasons for the observed discrepancy between the measured and predicted resistance values may be due to solder-conductor cross section mismatch as well measurement errors during testing and solder shape mismatch. To improve modeling prediction results in subsequent studies, geometry modification as well as acquiring more detailed Sn-Bi material properties related to physics of electromigration are recommended. Also, more

testing data points are required to verify modeling results for a range of current density and temperatures of Sn-Bi solder joints.

## REFERENCES

1. I. Blech, "Electromigration in thin aluminum films titanium nitride", *Journal of Applied Physics*, vol 47, 1976, pp. 36-53.
2. I. Blech, C. Herring, "Stress generation by electromigration" *Applied Physics Lecture*, Vol 29, 1976, pp. 131.
3. I. Blech, K. L. Tai, "Measurement of stress gradient generated by electromigration" *Applied physics Letter*, vol. 30, 1977, pp. 387.
4. R. Kirgheim, U. Kaeber, "Atomistic and computer modeling of metallization failure of integrated circuit by electromigration" *Journal of Applied Physics*, vol. 70, 1991, pp .1.
5. R. Kirchheim, "Stress and electromigration in Al-lines of integrated circuits" *Acta Metall. Mater.*,vol. 40, 1992, pp. 309-323.
6. S. Rzepka, E. Meusel, M. A. Korhonen, and C.-Y. Li, "3-D finite element simulator for migration effects due to various driving forces in interconnect lines," *AIP Conference Proceedings*, vol. 491, 1999, pp. 150.
7. Dandu P, Fan XJ, Liu Y. Some remarks on finite element modeling of electromigration in solder joints. *IEEE 60th Electronic Components and Technology Conference (ECTC)*, Las Vegas, NV, USA, 2010.
8. Dandu P, Fan XJ. "Assessment of current density singularity in electromigration of solder bumps." *IEEE 61st Electronic Components and Technology Conference (ECTC)*, Orlando, FL, USA, 2011.
9. *SpaceClaim User's Guide*, ANSYS Corporation, 2007.
10. X.Gu, Y.C.Chan, Electromigration in line type Cu/Sn-Bi/Cu solder joints, *JEM*, 37, 1721-1726 (2008).
11. Y. Liu, K.N. Tu, Low melting point solders based on Sn, Bi, and In elements, *Materials Today Advances*, 8 (2020) 100115.
12. E. Antonova, D. Looman, Finite element for electromigration analysis, *IEEE 67<sup>th</sup> electronic components and technology conference*, 2017.
13. C. Zhen, F. Xuejun, Z. Guopi, Implementation of general coupling model of electromigration in ANSYS, *IEEE 70<sup>th</sup> Electronic components and technology conference (ECTC)*, 2020.
14. H. Kang, S. Rajendran, J. Jung, Low melting temperature Sn-Bi solder, effect of alloying and nanoparticle addition on the microstructural, thermal, interfacial bonding and mechanical characteristics, *metals*, 2021.

15. Ansys Mechanical User's guide, ANSYS Corporation, 2013.
16. M. Nasir, electromigration danafe in lead free solder joints prepared using metallic nanoparticle doped flux, PhD thesis, University of Kuala Lumpur, 2007.